29th Congress of the International Council of the Aeronautical Sciences
St. Petersburg, Russia; September 7-12, 2014

SEPARATED LAMINAR SHEAR LAYER TRANSITION OVER A TWO-DIMENSIONAL BUMP

Yu-Long Ba, Chong Pan, Jin-Jun Wang*
Fluid Mechanics Key Laboratory of Education Ministry, Beijing University of Aeronautics and Astronautics, Beijing 100191, P. R. China
***Corresponding author: jjwang@buaa.edu.cn**

Keywords: *Bump, Laminar flow separation, Separation bubble, Shear layer transition*

Abstract

The laminar boundary layer separation over a two-dimensional bump is experimentally investigated in a water channel with hydrogen-bubble visualization and particle image velocimetry (PIV) techniques, focusing on the characteristics of separated shear layer, the evolution of flow structure and the development of unstable disturbances. It is shown that the separation point, to a large extent, depends on the geometry of the bump, while the reattachment point is mainly affected by Reynolds number. A quite long and narrow separation bubble with its vortex centre located very close to the reattachment point is observed when the laminar boundary layer separates over the bump. The shear layer transition begins as soon as the laminar boundary layer flow is separated, with the flow field perturbation increasing rapidly to a maximum value and then decreasing slowly along the streamwise direction. The formation and shedding of two-dimensional spanwise vortex structures are observed along the shear layer due to Kelvin-Helmholtz instability. These spanwise vortices gradually lose their two-dimensionality and evolve into hairpin vortices downstream.

1 Introduction

The separation of a laminar boundary layer is a very prevalent flow phenomenon which widely exists in aerospace, fluid machinery and other practical engineering. Particularly for a low Reynolds number airfoil at large angles of attack, the flow separation usually occurs at the leeward side of the airfoil due to the presence of strong adverse pressure gradient forming a recirculation region. It is commonly known as the separation bubble, which has been the subject of many studies in the past.

The flow structure over the suction surface of an airfoil with a large angle of attack at low Reynolds numbers can be simulated by the two-dimensional separation of a bump. The most important feature of this flow separation is that the separation point is not fixed, and is usually influenced by a series of factors such as the bump shape, flow parameters, surface roughness and other factors. So far, investigation on turbulent boundary layer separation has provided detailed experimental data and numerical simulation results [1-4].

However, the two-dimensional laminar boundary layer separation over a bump is less studied. According to the numerical simulation of separation instability over a bump by Marquillie and Ehrenstein [5], the size of the laminar separation bubble increases with Reynolds number when Reynolds number based on the bump height and free stream velocity is less than about 1200. The opposite is true when Reynolds number is more than 1200. For flow over backsteps, this critical Reynolds number is about Re = 820 based on the free stream velocity and step height [6].

In this paper, with hydrogen-bubble visualization and particle image velocimetry (PIV) techniques, the laminar separation over the two-dimensional bump is investigated. Focusing on the characteristics of laminar boundary layer separation and the evolution and

development of flow structure, the aim of this work is to deepen understanding of the mechanism of the separated shear layer transition downstream of the bump.

2 Experimental Set-up

The present experiment is conducted in a low-speed circulating water channel with test section of 600 mm × 600 mm × 4800 mm (height × width × length) at Beijing University of Aeronautics and Astronautics. The streamwise turbulence intensity is no more than 0.8% for the freestream velocity lower than 20 cm/s. Its bottom and two lateral walls are made of transparent Plexiglas, so that the flow field can be observed and photographed from any side of the water channel.

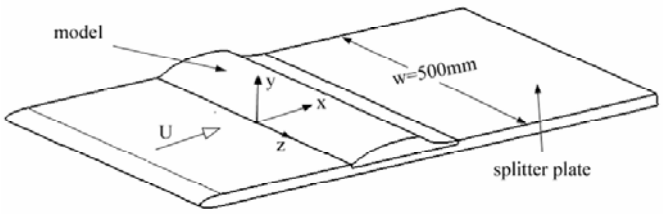

Fig. 1 Experimental model

The experimental model was a two-dimensional aluminum alloy bump fixed horizontally on a Plexiglas flat plate, as shown in Fig. 1. The configuration of this model has been used by many researchers [1,7-8], and the size is scaled to 1/3 of the original dimensions. The characteristic reference chord length of the model was defined as the streamwise length of the bump, i.e. c =140 mm. The height and width of the bump are h = 17.9 mm and w = 500 mm, respectively. The leading and trailing edges of the model were smoothly mounted on a water tunnel splitter plate which was constructed from Plexiglas. The splitter plate has a size of 2000 mm × 500 mm × 15 mm (length × width × thick), and is horizontally positioned 200 mm above the bottom of the water channel. The leading edge of the splitter-plate, which has a 4:1 elliptical modification to avoid leading-edge separation, was 800 mm upstream of the bump model's leading edge. The experimental free stream velocity is U_∞ = 32 mm/s to 82 mm/s, and the Reynolds number based on U_∞ and the bump height h is in the range of Re = 450 to 1200. Without the bump, flow over the flat plate is laminar boundary layer for the cases investigated in the present experiments as that measured by Pan et al. [9] and He et al. [10].

The flow field was measured by the two-dimensional PIV system. The field of view was illuminated by a light sheet from a successive laser. The tracer particles were hollow glass beads with diameter 5~10μm and average density 1.05 g/mm^3. The flow field of test-section was captured using a high speed CCD camera with a spatial resolution of 640 × 480 pixels and 8 bits in gray level. The sampling frequency of the high speed CCD was 100 Hz with the exposure time 5 ms. Ten thousand frames were recorded continuously in one group and three groups were taken for one case. The images were dealt with the cross-correlation calculation between two successive images. Gaussian peak fit was applied to enhance the resolution of cross-correlation peak identification to a sub-pixel level. The sizes of the interrogation window and search window were set to 32 × 16 pixels and 16 × 8 pixels, respectively. Multi-grid iteration with window deformation was also used to improve the trace accuracy of the interrogation window. Ultimately, the relative uncertainty in measured velocity would be less than 1% [9].

3 Results and Discussion

3.1 Mean Flow Characteristics

Figure 2(a) shows the time-averaged location of the separation region over the two-dimensional bump for Re = 700. The recirculation border, the streamline from the separation point, divides the time averaged flow field into two zones: the outer zone and recirculation zone. The recirculation zone is divided by the zero streamwise velocity line into two parts, and the back flow zone is formed between the zero streamwise velocity line and the wall. According to the two-dimensional laminar boundary layer separation criterion by Prandtl,

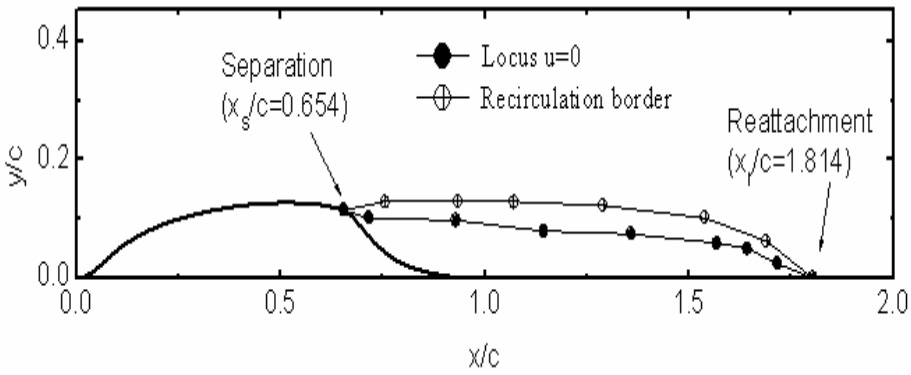

(a) Locus of zero longitudinal velocity and separation bubble border for *Re* = 700

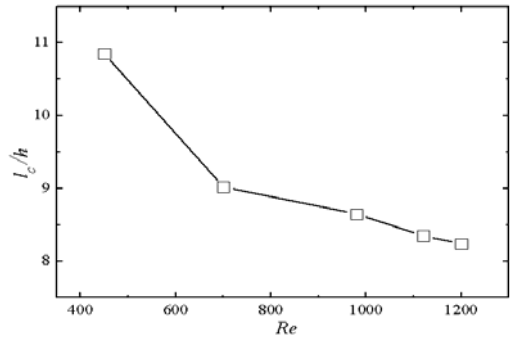

(b) Variation of separation bubble length with Reynolds number

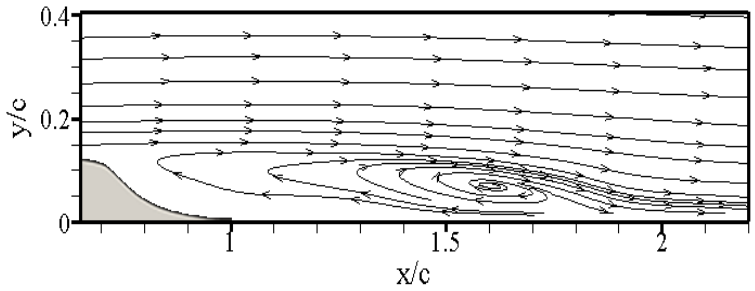

(c) Time-averaged streamline for *Re* = 700

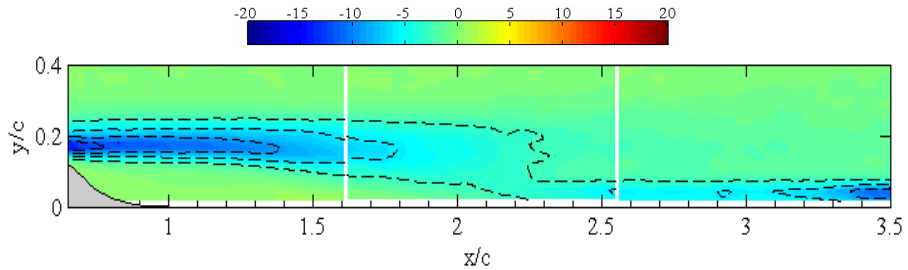

(d) Time-averaged spanwise vorticity $\omega_z c/U_\infty$ for *Re* = 700

Fig. 2 Mean flow field downstream of the bump

the vertical mean velocity in the wall at the separation point should be zero. With this criterion, we obtain that the separation point is located at about *x*/*c* = 0.654, and a long and narrow bubble is formed at the leeside of the bump, and then reattaches at *x*/*c* = 1.814 (Fig. 2a).

It is shown in Fig. 2(b) that the mean separation bubble length decreases with the Reynolds number, meaning that the separated shear layer undergoes transition prior to

reattachment [6]. Therefore, this ensures that the experiment is conducted in proper condition so as to investigate the separated shear layer transition.

Figure 2(c) shows the time-averaged streamlines for Re = 700. For the Reynolds numbers studied in the present paper, it is observed that the extremely narrow and long time-averaged separation bubbles are formed at the leeside of the bump for the laminar boundary layer separation. The shape of these separation bubbles is not only quite different from turbulent separation bubbles [1-2], but also different from laminar separation bubbles over the suction surface of a low Reynolds number airfoil at a high angle of attack [11]. The turbulent separation flow will soon reattach after separation, thus forming a short length separation bubble. The laminar separation over the airfoil surface is usually influenced by its trailing edge, thus a long separation bubble will not be formed.

Figure 2(d) shows the time-averaged vorticity field for Re = 700. It can be seen that the high concentration regions of negative vorticity mainly appear in the separated shear layer, while the vorticities are weaker above the shear layer and between the shear layer and the wall. The strength of vorticity in the shear layer gradually decreases with the increase of the streamwise position, and the strong shear induced by flow separation gradually becomes weaker after the reattachment. Similar phenomenon also occurs for other Reynolds numbers.

3.2 Fluctuation Characteristics

Figure 3 shows profiles of Reynolds shear stress at Re = 700. The Reynolds shear stress between the shear layer and the wall increases slowly after separation, then a rapidly increase is observed at x/c = 1.2-1.8, and its maximum value appears at x/c = 2.0. The distribution of Reynolds shear stress has a strong regularity, which increases in the separation region, reaches the maximum at x/c = 2.0 and then decreases. Practically, the maximum value of $-\overline{u'v'}/U_\infty^2$ is usually located at y/c = 0.13-0.18.

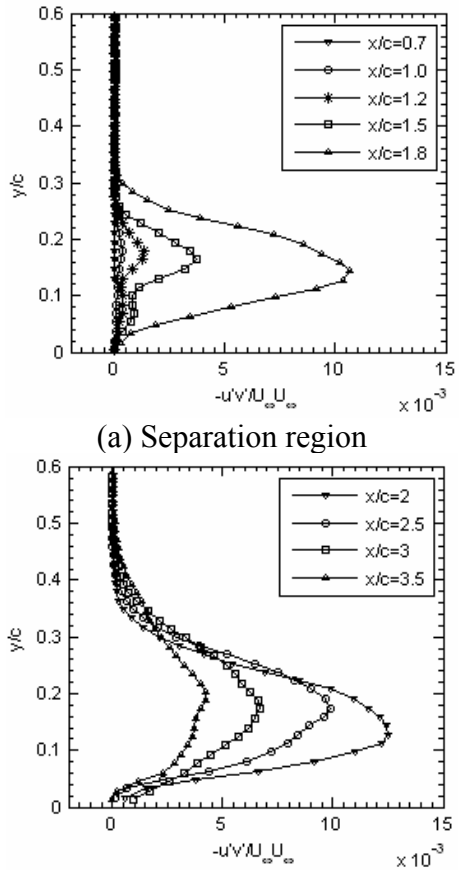

(a) Separation region

(b) Downstream of the reattachment point

Fig. 3 Profiles of Reynolds shear stress, $-\overline{u'v'}/U_\infty^2$ at Re = 700

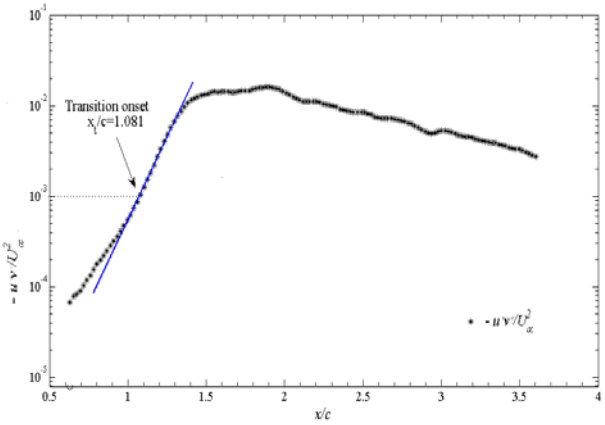

Fig. 4 Methods to detect the transition onset for Re = 1120

In the past years, Reynolds shear stresses $-\overline{u'v'}/U_\infty^2$ have been used as the standard to determine the start of the transition process (x_t) in laminar boundary layer separation flow [4,11-12]. According to these studies, the present transition onset is defined as the region where the threshold of 0.001 is reached. It can be seen

from Fig. 4 that the transition onset is located at x_t/c = 1.081 for Re = 1120 in this investigation.

3.3 Evolution of Vortex Structure

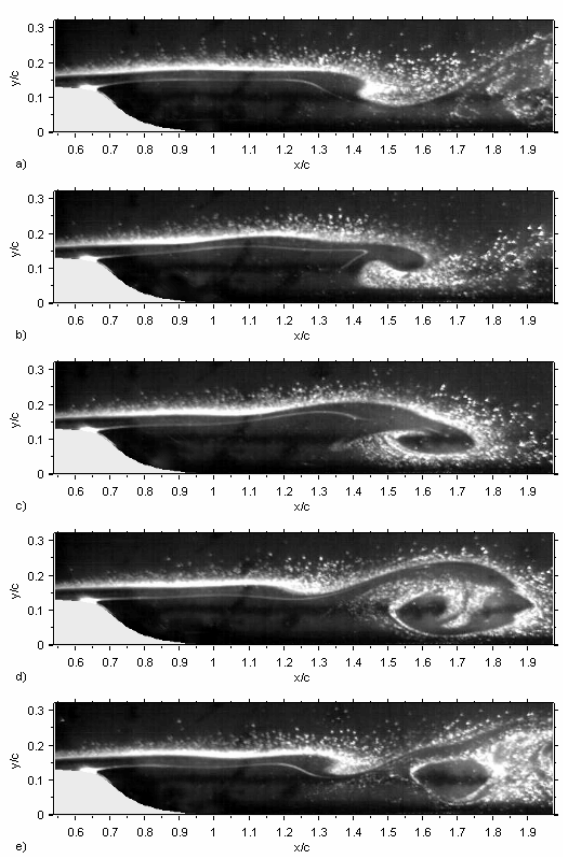

Fig. 5 Vortex shedding visualization of the shear layer for Re = 700. Time interval between two images is Δt = 0.69 s. The platinum wire is positioned at x/c = 0.5, y/c = 0.16.

In the present experiment, the spanwise vortices are observed periodically generating from the shear layer downstream of the bump. Figure 5 shows the evolution of the vortex structures in a vortex shedding cycle for Re = 700. The shear layer is disturbed and becomes unstable at the location around x/c = 1.3 at time t_0 (Fig. 5a), which corresponds to the rapid growth of the Reynolds stress at x/c = 1.2. The disturbance is further amplified under the effect of shear at time $t_0+\Delta t$ (Fig. 5b). The vortex structure with negative vorticity (clockwise rotation), formed at x/c = 1.5-1.8, develops into a complete vortex structure, and then continues to advect downstream (Fig. 5c). The formation of spanwise vortex shedding from the shear layer develops into an independent vortex structure in the next time interval (Fig. 5d). A new formation process starts in Fig. 5(e). According to the evolution of the vortex structure, the reattachment point is probably located at x/c = 1.5-2.0, consistent with the mean value x/c = 1.814 obtained from PIV data (Fig. 2a).

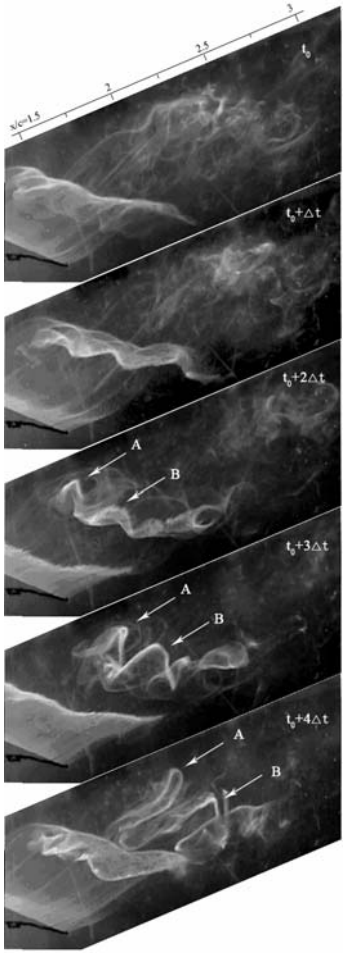

Fig. 6 Generation process of hairpin vortices for Re = 1200. Time interval between two images is Δt = 0.55 s. The platinum wire is positioned at x/c = 0.5, y/c = 0.16.

The transverse vortices have good two-dimensionality at the initial stage of their formation, with the vortex lines extending directly along the spanwise axis. In the downstream convection process, they gradually lose their two-dimensional nature and rapidly evolve into hairpin vortices due to the increased disturbance. Hairpin vortices, which are also known as horseshoe vortices, Λ-vortices and ring-like vortices etc., have been accepted as key structures in a turbulent boundary layer and are strongly associated with turbulent self-sustaining mechanisms [13-15].

In this paper, the hairpin vortices, which evolved from transverse vortex structures shedding from the shear layer, can be observed for all cases investigated. The large-scale hairpin vortices are formed with nearly fixed locations for low Reynolds number cases. The small-scale, irregular hairpin vortices are observed due to the much more chaotic flow field. Figure 6 gives an example of the generation process of two hairpin vortices A and B from a transverse vortex structure in one vortex shedding cycle for Re = 1200. The bright lines in the visualization images are the amalgamated hydrogen bubbles due to the swirling motion, thus indicating the vortex cores. It is shown that the transverse vortex core initially exhibits good two-dimensionality at the moment t_0. As it advects downstream, a small non-uniformity appears in the vortex core, which is soon amplified due to vortex instability of multi-inflection points in the spanwise direction at $t_0+\Delta t$. Part of the transverse vortex can be accelerated sufficiently, thus protruding downstream at $t_0+2\Delta t$. Owing to the background mean shear, the flow acceleration is always coupled with lift-up motion. Therefore, the downstream protruded part lifts up to be further accelerated, while its neighboring parts are still retarded in the near-wall region. At $t_0+3\Delta t$, two Λ-shaped structure indicated by arrows A and B are moving away from the original vortex. Their legs undergo continuous streamwise stretching while their heads bend back due to the different heights they are located at. Further downstream at $t_0+4\Delta t$, they eventually form two hairpin vortices. The similar evolution is also reported by Chang et al. [16] for flow past an open cavity.

Figure 6 shows that, for the case of Re = 1200, the three-dimensionality of the transverse vortex appears at x/c = 1.5, downstream of the transition onset (x_t/c = 1.338). This phenomenon is also found for other cases. Therefore, the hairpin vortices observed in this investigation are formed in the boundary layer transition region, which has the same generation mechanism in the experimental study of cylinder wake-induced flat plate boundary layer transition by Pan et al. [9], from the three-dimensional instability in the early transition process. Svizher and Cohen [14] proposed that the formation of hairpin vortices from the perturbed vortex evolution exits a general mechanism, of which two basic conditions are the initial vortex disturbance being large enough and the existence of the background shear. It is visible that the formation of the hairpin vortices observed in the present investigation meets these two requirements.

4 Conclusions

The characteristics of separated shear layer, the evolution of flow structure and the development of unstable disturbances over a two-dimensional bump are experimentally investigated for Re = 450 to 1200. Particular attention is paid to the dynamics of the separated shear layer evolution. The following conclusions can be made.

Firstly, the separation point depends mostly on the geometry of the bump, while the reattachment point is largely affected by the Reynolds number. A very long and narrow separation bubble with its vortex centre very close to the reattachment point is observed when the laminar boundary layer separated on the leeside of the bump.

Secondary, the flow transition begins when the laminar boundary layer separates, with flow field perturbation increasing rapidly to a maximum and then declining slowly along the streamwise direction.

Thirdly, the formation and shedding of two-dimensional spanwise vortex structures are observed along the shear layer due to Kelvin-Helmholtz instability. These spanwise vortices gradually lose their two-dimensionality and evolve into hairpin vortices downstream.

References

[1] Greenblatt D, Paschal KB, Yao CS., Harris J, Schaeffler N and Washburn A. A separation control CFD validation test case part 1: Baseline and steady suction. *AIAA Journal*, Vol. 44, pp 2820-2830, 2006.

[2] Loureiro JBR, Pinho FT and Freire APS. Near wall characterization of the flow over a two-dimensional steep smooth hill. *Experiments in Fluids*, Vol. 42, pp 441-457, 2007.

[3] Houra T and Nagano Y. Turbulent heat and fluid flow over a two-dimensional hill. *Flow Turbulence Combust*, Vol. 83, pp 389-406, 2009.

[4] McAuliffe BR and Yaras MI. Passive manipulation of separation-bubble transition using surface modifications. *Journal of Fluid Engineering*, Vol. 131, pp 0212011, 2009.

[5] Marquillie M and Ehrenstein U. On the onset of nonlinear oscillations in a separating boundary-layer flow. *Journal of Fluid Mechanics*, Vol. 490, pp 169-188, 2003.

[6] Sinhua SN, Gupta AK and Oberai MM. Laminar separating flow over backsteps and cavities, Part 1: backsteps. *AIAA Journal*, Vol. 19, pp 1527-1530, 1981.

[7] Morgan PE, Rizzetta DP and Visbal MR. Large-eddy simulation of separation control for flow over a wall-mounted hump. *AIAA Journal*, Vol. 45, pp 2643-2660, 2007.

[8] Avdis A, Lardeau S and Leschziner M. Large eddy simulation of separated flow over a two-dimensional hump with and without control by means of a synthetic slot-jet. *Flow Turbulence Combust*, Vol. 83, pp 343-370, 2009.

[9] Pan C, Wang JJ, Zhang PF and Feng LH. Coherent structures in bypass transition induced by a cylinder wake. *Journal of Fluid Mechanics*, Vol. 603, pp 367-389, 2008.

[10] He GS, Wang JJ and Pan C. Initial growth of disturbance in the boundary layer influenced by a circular cylinder wake. *Journal of Fluid Mechanics*, Vol. 718, pp 116-130, 2013.

[11] Burgmann S and Schroder W. Investigation of the vortex induced unsteadiness of a separation bubble via time-resolved and scanning PIV measurements. *Experiments in Fluids*, Vol. 45, pp 675-691, 2008.

[12] Lang M, Rist U and Wagner S. Investigations on controlled transition development in a laminar separation bubble by means of LDA and PIV. *Experiments in Fluids*, Vol. 36, pp 43-52, 2004.

[13] Robinson SK. Coherent motions in the turbulent boundary layer. *Annual Review of Fluid Mechanics*, Vol. 23, pp 601-639, 1991.

[14] Svizher A and Cohen J. Holographic particle image velocimetry measurements of hairpin vortices in a subcritical air channel flow. *Physics of Fluids*, Vol. 18, pp 014105, 2006.

[15] Adrian RJ. Hairpin vortex organization in wall turbulence. *Physics of Fluids*, Vol. 19, pp 041301, 2007.

[16] Chang K, Constantinescu G and Park SO. Analysis of the flow and mass transfer processes for the incompressible flow past an open cavity with a laminar and a fully turbulent incoming boundary layer. *Journal of Fluid Mechanics*, Vol. 561, pp 113-145, 2006.

Acknowledgments

This work is supported by the National Natural Science Foundation of China (Grant Nos. 11002015 and 10832001).

Copyright Statement